Multi-Resolution Analysis Wavelet PI Stator Resistance Estimator for Direct Torque Induction Motor Drive

EHAB H.E. BAYOUMI
Power Electronics and Energy Conversion Department,
Electronics Research Institute (ERI),
Cairo 12622, Egypt
E-mail: ehab-bayoumi@lycos.com

Abstract: - To improve the overall dynamic performance of induction motor in direct torque control (DTC), a novel method of stator resistance estimation based on multi-resolution analysis wavelet PI controller is presented. This estimation method is anchored in an on-line stator resistance correction regarding the variation of the stator current estimation error. The main purpose is to adjust precisely the stator resistance value relatively to the evolution of the stator current estimation error gradient to avoid the drive instability and ensure the tracking of the actual value of the stator resistance. The multi-resolution wavelet controller process the error input with the gains depending on the level of decomposition employed. In order to limit the number of gains, this paper analyzes multi-resolution wavelet controller with a single gain constant. A separate fractional order integrator unit which enhances the controller performance with additional flexibility of tuning and also offers better steady state performance of the motor is introduced. The simulation results show that the proposed method can reduce the torque ripple and current ripple, superior to track the actual value of the stator resistance for different operating conditions.

Key-Words: - Direct Torque Control, multi-resolution wavelet analysis, PI Controller, Stator Resistance Estimator.

1 Introduction

Due to its simple structure, good dynamic performance, robustness and ability to achieve fast response of flux and torque, the direct torque control (DTC) strategy has attracted more and more interest in recent years [1] and it has been widely used to overcome the problems of variable switching frequency and high torque ripples at low speeds [2-5].

However, the stator resistance change can significantly degrade the performance of a direct torque controlled induction motor since the stator resistance is additionally required for stator flux and torque estimation in the basic configuration of DTC. In fact, one of the main problems of the DTC of induction motor drives is the variation of the stator resistance which is affected mainly by the change in motor temperature [1]. This variation which is usually in the range of 0.75-1.7 times its nominal value [6], deteriorates the performance of the drive by introducing errors in the estimated flux linkage's magnitude and its position and hence in the electromagnetic torque [6]. At low speed, this effect is important for a given load torque. And if the value of the stator resistance used in the DTC controller is less than the actual value, the developed flux and torque will be decreased. Moreover, using greater value of the stator resistance in controller than its real value may lead to instability [1].

Elsewhere, an accurate value of the stator resistance is of crucial importance for correct operation of a sensorless drive in the low speed region, since any mismatch between the actual value and the value used within the speed estimator may lead not only to a substantial speed estimation error but to instability as well [3, 7]. As a consequence, numerous online schemes for stator resistance estimation have been proposed in the recent past years.

An adaptive stator resistance compensation scheme applied to eliminate the stator resistance parameter sensitivity using only the existing stator current feedback has been presented [6]. A procedure for finding the stator current phasor command from the torque and the stator flux linkage commands is derived to realize the adaptation

scheme. Stator current phasor command derived from this procedure is independent of stator and rotor resistances of the induction motor in DTC control.

Proportional-integral (PI) or integral (I) controllers were used also for an online stator resistance identification where an updated stator resistance value is obtained through an adaptive mechanism. In principle, two distinct subcategories of adaptor mechanism exist. The stator resistance PI compensator is based on on-line stator resistance correction regarding the variations of the stator current magnitude, which must be constant value when the stator flux and motor torque are constant [1]. The method proposed in [8] used back electromotive force detector which decouples direct component of stator flux from the corrupting effects of the stator resistance, producing an ideal signal for the adaptation algorithm. In addition, the quadrature component provides a near instantaneous estimate of the stator resistance. Another stator resistance identification algorithm based on the steady-state power flow between stator and rotor through the air gap has been presented [9]. The air gap power was calculated using the steady-state value of the estimated torque. Then, the stator resistance was estimated using the difference between these two steady-state powers. The reactive power is evaluated first, stator and rotor flux are calculated next, and electromagnetic torque is then evaluated [10]. An explicit expression for stator resistance calculation is finally derived, as a function of the previously calculated quantities. A simple but effective stator resistance compensated DTC method for induction motor operating at low speed has been proposed in [11].

In observer-based systems the error quantity, which serves as an input into the stator resistance adaptation mechanism, is determined with the difference between the measured and the observed stator current components [12-15]. The problem of simultaneous online estimation of both rotor and stator resistance based on the measurements of rotor speed, stator currents and stator voltage has been addressed [12]. They have shown that both stator and rotor resistance estimates converged exponentially to the true values for any unknown values of the two stator and rotor resistances. The error quantity is formed in such a way that the stator resistance identification is independent of the total leakage inductance [15]. In MRAS-based systems [13-17], the choice of the error quantity is more versatile. [3, 13] presented a sensorless induction motor drive with stator resistance on-line estimation. This estimation method is based on current measurement only, and is well defined under any steady state condition regardless of the load level. This precise and reliable resistance estimator makes the system particularly suitable for low speed operation. Another resistance estimation method for speed sensorless purposes using a full order observer is proposed in [14]. Here the stator resistance estimation is based on a two-time scale approach, and the error between the measured and observed stator current is used for the parameter tuning. While the scheme in [16] operates in the rotating reference frame and the error quantity is determined with the difference between the rotor flux *dq*-axis components obtained from the voltage and current models. The error quantity based on active power is showed in [17].

The third major category of stator resistance online identification schemes relies on utilization of artificial intelligence techniques in the process of stator resistance adaptation. Artificial neural networks (ANNs) [18-23], fuzzy logic (FL) control [2, 21-23], or neurofuzzy control [24], were used for this purpose. Principally, schemes with ANNs can be regarded as a special subcategory of the first group of methods, where an explicit calculation of the stator resistance is replaced with a neural network-based approximation. Similarly, FL-based methods can be looked at as a subcategory of the second group of methods, where the classical adaptive mechanism (PI or I controller) is replaced with an FL adaptive mechanism. A stator resistance identifier using a recurrent ANN which is found to be much superior to PI and fuzzy estimator, both in terms of dynamic estimation times and convergence problems has been proposed [18].

The fuzzy stator resistance updating analyzed the performances of a DTC scheme with a stator resistance fuzzy identification [2]. The proposed fuzzy estimator improves the stator flux estimation accuracy leading to a smooth trajectory of the flux stator vector and therefore reducing the torque ripples. This estimator is particularly suited in applications needing high torque at low speed and improves the performance of the control strategy in applications where thermal impact on resistance variation is no more negligible. A quasi-fuzzy method of on-line stator resistance estimation has been described in [24]. The resistance value is derived from the stator winding temperature estimation as a function of the stator current and

frequency through an approximate dynamic thermal model of the machine.

Owing to the wavelet transform behaving good localization property in both time and frequency space and multi-scale property [25-30]. In [27] the wavelet function is adopted as the basic function of neural network, that is, the wavelet network (WN) function. Compared with neural network, wavelet network has four merits: self-construction network, partial retrieval of approximated function, fast convergence and escaping local minima. It identify the stator resistance of induction motor on-line using the wavelet network, and realize the accurate tracking of the stator resistance, improving the DTC system's. The wavelet-based multi-resolution controller is introduced in [28]. In [29, 30] the main objective is to develop and implement a wavelet based multi-resolution PID controller in real-time for precise speed control of IPM motor drives under system uncertainties. The controller is based on the multi-resolution decomposition property of the discrete wavelet transform (DWT) of the error signal between the command and actual speeds. The control signal is generated by adding the wavelet transformed coefficients of the error signal of different frequency sub-bands of the DWT tree after scaled by their respective gains. The proposed wavelet based PID controller for IPM motor drives is successfully implemented in real-time but it needs to be enhanced against system uncertainties.

This paper is concerned with a relatively simple solution to track the stator resistance so that the performance degradation and a possible instability problem can be avoided. A new robust and simple multi-resolution analysis wavelet PI estimator using the measured stator currents is applied. The paper is organized as follows: in section 2 presents the idea, and mathematical model of DTC for induction motor drive. The wavelet transformation and the multi-resolution analysis wavelet PI controller is introduced, modelled and explained in section 3.The overall system and modelling of the proposed controller are given in section 4. In section 5 the simulation results are realized by using MATLAB-SIMULINK package. The performance and robustness of the proposed PI estimator are shown and discussed via dynamic simulation studies. Conclusions and comments are established in section 6.

2 DTC for Induction Motor Drive

Since DTC has evolved from a particular control strategy to a wide concept that employs a broad range of control solutions. Many existing schemes for DTC are introduced in literature. It achieved high-performance torque and flux control by using modern control techniques. The DTC principle is: simultaneous and decoupled control of torque and stator flux. It is achieved by direct adjustment of the stator voltage, in accordance with the torque and flux errors, without intermediate current control and/or decoupling network.

The DTC strategy introduced in this paper is based on the direct control of stator flux and electromagnetic torque through stator voltage vector selection. The conventional block diagram of the DTC for three-phase induction motor with a speed control loop is shown in Fig.1. This method presents the advantage of a very simple control scheme of stator flux and torque by two hysteresis controllers, which give the input voltage of the motor by selecting the appropriate voltage vectors of the inverter through a look-up-table in order to keep stator flux and torque within the limits of two hysteresis bands.

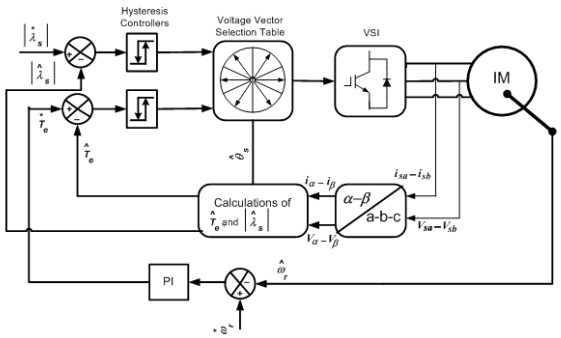

Fig. 1. Conventional block diagram of DTC for Induction motor drive system.

Using the α-β coordinate system, the time-varying state space model of the induction motor can be written as given:

$$\frac{di_{S\alpha}}{dt} = -\frac{1}{\sigma}(\gamma+\eta)i_{S\alpha} - \omega i_{S\beta} + \frac{1}{\sigma L_S L_r}\lambda_{S\alpha} + \frac{1}{\sigma L_S}V_{S\alpha} \quad (1)$$

$$\frac{di_{S\beta}}{dt} = \omega i_{S\alpha} - \frac{1}{\sigma}(\gamma+\eta)i_{S\beta} + \frac{1}{\sigma L_S L_r}\lambda_{S\beta} + \frac{1}{\sigma L_S}V_{S\beta} \quad (2)$$

$$\frac{d\lambda_{S\alpha}}{dt} = -R_S\, i_{S\alpha} + V_{S\alpha} \quad (3)$$

$$\frac{d\lambda_{S\beta}}{dt} = -R_S\, i_{S\beta} + V_{S\beta} \quad (4)$$

$$\frac{d\omega}{dt} = \frac{3p^2}{2J}(\lambda_{S\alpha}\, i_{S\beta} - \lambda_{S\beta}\, i_{S\alpha}) - \frac{p}{J}T_L - \frac{B}{J}\omega \quad (5)$$

where

$\sigma = 1 - \frac{L_m^2}{L_S L_r}$, rotor time constant= $\eta = \frac{R_r}{L_r}$ and stator

time constant= $\gamma = \frac{R_S}{L_S}$. The α and β components of the stator flux can be obtained through the integration of the difference between the stator voltage and voltage drop in the stator resistance as:

$$\lambda_{S\alpha} = \int (V_{S\alpha} - R_S\, i_{S\alpha})\, dt \text{, and}$$

$$\lambda_{S\beta} = \int (V_{S\beta} - R_S\, i_{S\beta})\, dt \quad (6)$$

Hence, the flux linkage phasor is expressed as follows:

$$\left|\overline{\lambda_S}\right| = \sqrt{\lambda_{S\alpha}^2 + \lambda_{S\beta}^2} \text{ and } \theta_S = \angle\overline{\lambda_S} = \tan^{-1}\left(\frac{\lambda_{S\beta}}{\lambda_{S\alpha}}\right) \quad (7)$$

And the electromagnetic torque is given by:

$$T_e = \frac{3p}{2}(i_{S\beta}\,\lambda_{S\alpha} - i_{S\alpha}\,\lambda_{S\beta}) \quad (8)$$

Similar transformation is applied to voltages and flux linkages. It is assumed that the voltages and currents are balanced, and hence zero sequence voltages and currents are absent. To obtain uniform rotating stator flux, the motor voltages have to be rotated uniformly too as shown in Fig. 2. This requires continuously variable stator voltages with infinite steps, which is not usually met by the inverter due to the fact that it has only eight switching states and its switching frequency is limited by thermal factors. The limited states of the inverter create distinct discrete movement of the stator voltage phasor, V_s, is the resultant of $V_{s\alpha}$ and $V_{s\beta}$. In spite of this limitation, almost continuous and uniform flux linkage phasor is feasible with these discrete voltage states due to their integration over time as given in Eq. (6). Stator resistance is the only motor parameter that affects all the key variables as shown in Eqs. (6-8).

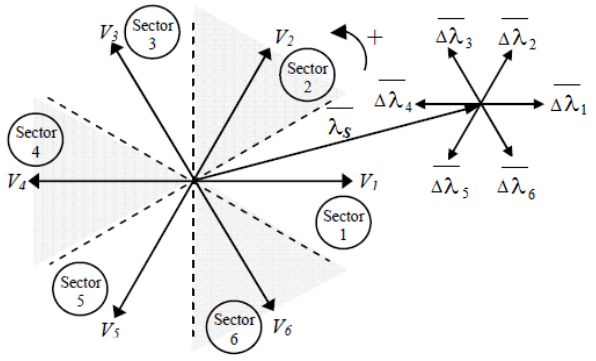

Fig. 2. Inverter voltage space vector.

Table 1 summarizes the combined action of each inverter voltage space vector on both the stator flux amplitude and the motor torque. In this table, a single arrow means a small variation, whereas two arrows mean a larger variation. As can be seen, an increment of torque (↑) is obtained by applying the space vectors V_{k+1} and V_{k+2}, irrespective of the motor speed direction. Conversely, a decrement of torque (↓) is obtained by applying V_{k-1} or V_{k-2}. The space vectors V_k, V_{k+3} and the zero voltage space vectors modify the torque in accordance with the motor speed direction as specified in Table 1.

Table 1. Stator flux and torque variations due to the applied inverter voltage space vectors

	V_{k+1}	V_{k-1}	V_k	V_{k+1}	V_{k+2}	V_{k+3}	$V_{0.7}$
λ_S	↓	↑	↑↑	↑	↓	↓↓	↑↓
T_e (ω > 0)	↓↓	↓↓	↓	↑	↑	↓	↓
T_e (ω < 0)	↓	↓	↑	↑↑	↑↑	↑	↑

3 Wavelet Transform

A wavelet, in the sense of the discrete wavelet transform, is an orthogonal function which can be applied to a finite group of data [25]. The transform is a convolution and the transforming function is orthogonal, a signal passed twice through the transformation remains unchanged, and the input signal is assumed to be a set of discrete time samples [25]. The wavelet transform decomposes the signal into different scales with different levels of resolution by dilating a single prototype function, the mother wavelet. The continuous wavelet transform (*CWT*) of *f(t)* is given by Eq.(9) [26].

$$CWT_\psi f(a,b) = W_f(a,b) = |a|^{\frac{1}{2}} \int_{-\infty}^{\infty} f(t)\,\psi^*\left(\frac{t-b}{a}\right) dt \quad (9)$$

Where a, $b \in R$, $a \neq 0$ and they are dilating and translating coefficients, respectively. The asterisk denotes a complex conjugate. The multiplication factor $|a|^{\frac{1}{2}}$ is for energy normalization purpose. The mother wavelet $\Psi(t)$ is scaled by a. The original signal can be completely reconstructed by a sample version of Wf(b,a), sampled in a dyadic grid ie. $a = 2^{-m}$ and $b = n2^{-m}$, and m, $n \in Z$, Z being the set of positive integers [26]. The discrete wavelet transform (*DWT*) can be defined by Eq.(10) [26].

$$DWT_\psi f(m,n) = \int_{-\infty}^{\infty} f(t)\,\psi_{m,n}^*(t)\, dt \quad (10)$$

Where, $\psi_{m.n}(t) = \psi(2^m t - n)$ is the dilated and translate version of the mother wavelet $\Psi(t)$.

3.1 Multi Resolution Wavelet Controller

The output of the multi-resolution wavelet controller is described in Eq.(11) [28], where *u(t)* is the controller output for error input *e(t)*, which is

decomposed in low frequency signal $e_1(t)$ with gain K_1, and high frequency signals $e_2(t) - e_N(t)$ with gain $K_2 - K_N$, respectively. For appropriate controller performance the controller gains $K_1 - K_N$, are to be tuned properly. The number of controller gains depends on the level of decomposition. Also the multi resolution analysis requires high and low pass filters to be cascaded, depending on the decomposition levels greater computational burden and execution time would be imposed.

$$u(t) = K_1 e_1(t) + K_2 e_2(t) + K_3 e_3(t) + ... + K_N e_N(t) \quad (11)$$

A multi-resolution wavelet controller requiring three controller gains for a proportional plus integral plus derivative (PID) controller and two for PI controller. The discrete wavelet decomposition has the form of transformation using quadrature mirror filters by which a signal sequence $x(k)$ is decomposed into n scales and the results of the decomposition operation is stored in the variable w_i shown in Eq.(12), where matrices G and H are the low and high pass filter, and signal sequence x is decomposed in n scale [29].

$$w_i = \left(Gx, GHx, GH^2x, ..., GH^{n-1}x, H^n x\right) \quad (12)$$

The decomposition expressed in Eq.(12) can be implemented using a recursive algorithm and with n scale discrete wavelet transform the input signal into n parts, each one representing a parameter of the dynamics of the signal [29]. The speed error signal is sampled and the sampled data is fed to an $1\times N$ array. For every new sample the data position is shifted from the N^{th} position towards the 0^{th} position, with the oldest data being discarded and the latest data being in the N^{th} position. As per the mother wavelet, Haar wavelet, the matrices G and H are given by Eqs.(13-14). Application of a three level decomposition wavelet transform for the error input sequence results in Eq.(15) [29], where, H^3x and GH^2x are as given in Eqs.(16-17), respectively, with $f(k)$ representing the low harmonic component of the input error and $g(x)$ expressing the higher harmonic component of the input error.

$$G = \frac{1}{\sqrt{2}}\begin{bmatrix}1 & 1\end{bmatrix} \quad (13)$$

$$H = \frac{1}{\sqrt{2}}\begin{bmatrix}1 & -1\end{bmatrix} \quad (14)$$

$$w_i = \left(Gx, GHx, GH^2x, H^3x\right) \quad (15)$$

$$f(k) = H^3x(k) = x_0(k) + x_1(k) + ... + x_{N-1}(k) \quad (16)$$

$$g(k) = GH^2x(k) = x_0(k) + x_1(k) + ... + x_{(N/2-1)}(k) - ..... - x_{N-1}(k) \quad (17)$$

$$f(k) = H^3x(k) = f(k-1) - x_0(k) + x_{in}(k) \quad (18)$$

$$g(k) = GH^2x(k) = g(k) - x_0(k) - x_{in}(k) + 2x_{(N/2)}(k) \quad (19)$$

An integrator term is added to eliminate the steady state error. The resulting multi-resolution PID controller is described in Eq. (18) [29], where $U(k)$ is the controller output at the k^{th} sampling instant, and K_p, K_i, K_d are the proportional, integral and differential gains, respectively. The integral term $I(k)$ is defined in Eq. (19), where T_s is the sampling time.

$$U(k) = K_p\ f(k) + K_d\ g(k) + K_i\ I(k) \quad (20)$$

$$I(k) = I(k-1) + T_s\ x_{in}(k) \quad (21)$$

In motor drive systems, the motor winding inductance persevere the damping requirements, leaving the derivative controller redundant. Also, the derivative controller acts as an amplifier for the noise signals and may lead to increase in noise and ripples in the controller output. The PI controller satisfies the needs of many controllers used in a motor drive system and it is usually implemented in practice significantly. The multi-resolution wavelet controller defined in Eq. (22), where the PI controller operation is obtained by neglecting the high frequency term which further simplifies the computations

$$U(k) = K_p\ f(k) + K_i\ I(k) \quad (22)$$

A significant advantage of the proposed controller over the wavelet controller proposed in [28-29] is the reduction in the computational burden and consequently the execution time. This merit is acquired as only two equations need to be solved for the determination of the high and low frequency components of the input discrete signal. This results in the elimination of the need of the low and high pass filtering at each level of decomposition. The low computational burden and execution time facilitate the further use of higher sampling and carrier frequency which leads to the reduction in harmonic losses

Fig. 3 shows the block diagram of a multi-resolution wavelet PI controller. The commanded and the actual value are compared and the resulting error x_{in} is fed to the 2- dimensional array. The necessary elements of the array are retrieved for the high and low frequency component computations. The low and high frequency component of the input error signal are represented by $f(k)$ and $g(k)$, respectively. These signals as per their gains are scaled and fed to the summer block. One more input to the summer block is the scaled integral of the error input. The output of the summer block represents the multi-resolution wavelet controller output. With the absence of the scaled high frequency signal, the summer output would represent the multi-resolution PI controller output.

To incorporate the merits of fractional order controller, multi-resolution wavelet PI speed controller with fractional order integrator, as defined in Eq. (23), has been proposed. The factorial order integrator term $I_{fo}(s)$ is defined in Eq. (24), where s is the Laplace operator and $0<\delta<1$ [25].

$$U(s) = K_p\ f(s) + K_i\ I_{fo}(s) \quad (23)$$

$$I_{fo}(s) = s^{-\delta} x_{in}(s) \quad (24)$$

4 Multi-Resolution Wavelet Analysis PI Stator Resistance Estimator

The proposed multi-resolution wavelet analysis PI estimator, which is designed to estimate the actual value of the stator resistance for different load torque and speed operating conditions, is shown in Fig. 4. The inputs of the wavelet network are the current error and the change in the current error, denoted by and, respectively. They are defined as

$$e(k) = \Delta I_s(k) = I_s^*(k) - I_s(k) \quad (25)$$

$$\Delta e(k) = e(k) - e(k-1) \quad (26)$$

$$I_s(k) = \sqrt{I_{s\alpha}^2(k) + I_{s\beta}^2(k)} \quad (27)$$

$$R_s(k) = R_s(k-1) + \Delta R_s(k-1) \quad (28)$$

where $I_s^*(k)$ is the stator command current and $I_s(k)$ is the actual current. The change in error is needed since the stator current magnitude changes nonlinearly as the stator resistance changes. The command current is determined using simulations and its value depends implicitly on the electromagnetic torque, the stator flux, and rotor speed commands, calculated using the conventional DTC. The relationship of $I_s^*(k)$ as a function of the stator flux, electromagnetic torque, and rotor speed commands can additionally be determined using a nonlinear function identification or a look-up table build upon experimental data. The output of the wavelet network gives the change in stator resistance $\Delta R_s(k)$ which is added to the previous value $R_s(k-1)$ to give an estimate for the actual value of the stator resistance $R_s(k)$, as it is shown in Fig. 4.

5 Results

The proposed system has been simulated by using MATLAB-SIMULINK package. To validate the performance of the multi-resolution analysis wavelet PI stator resistance estimator for a DTC of induction motor, the drive system has to be tested with and without stator resistance estimator. In Table 2, the induction motor parameters and the multi-resolution wavelet PI controller gains are given.

Table 2. Induction motor parameters and multi-resolution wavelet PI controller gains.

Motor Parameter	Value
Power	2.2 kW
Voltage, V	240V
Frequency, f	50 Hz
Number of poles, p	4 poles
Stator resistance, R_s	3.8 Ω
Rotor resistance, R_r	1.92 Ω
Stator self inductance, L_s	0.254 H
Rotor self inductance, L_r	0.254 H
Mutual inductance, L_m	0.228 H
Rotor inertia, J	0.0272 kg.m^2
Viscous friction coefficient, B	0.0742 N.m/rad/s
R_s, controller gain K_p	1.56
R_s, controller integeral gain K_i	0. 872

5.1 DTC for Induction Motor without Resistance Estimator

Instability in the DTC drive is occurred if the controller set stator resistance is greater than its actual value in the induction motor drive system [31]. Fig. 5(a) shows simulation results for a ramp stator resistance decrease from the nominal value (3.8 Ω) at 0.3 s. The drive system becomes unstable. This can as be explained as follows:

1- As the motor resistance decreases in the machine, the stator current increases for the same applied voltages. This leads to an increase of the stator flux and electromagnetic torque.
2- The controller has an opposite effect so that the increased currents, which are inputs to the system, cause increased stator resistance voltage drops in the calculator resulting in lower flux linkages and electromagnetic torque estimation. They are compared with their command values giving larger torque and flux linkages errors resulting in commanding larger voltages and hence larger currents leading to a run off condition as shown in Fig. 5(b-e)
3- In fact, from Fig. 5(f), it can be noticed that the stator resistance error causes improper flux estimation making the DTC perform poorly and leads to drive instability.

Consequently, the motor stator resistance adaptation is essential to overcome instability and to guarantee a linear torque amplifier in the direct torque controlled drive.

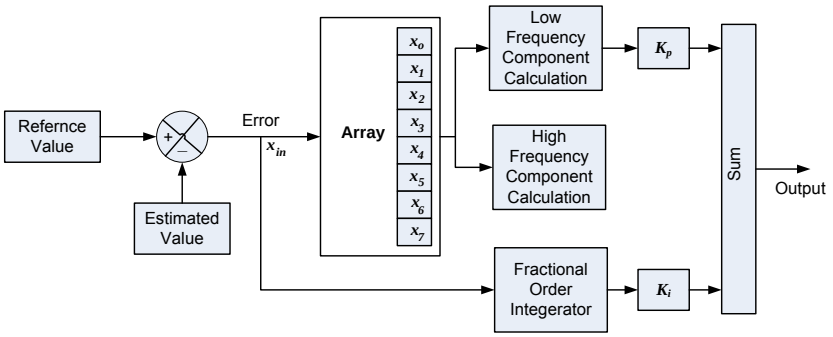

Fig. 3. Block diagram of multi-resolution wavelet PI controller and fractional order integrator.

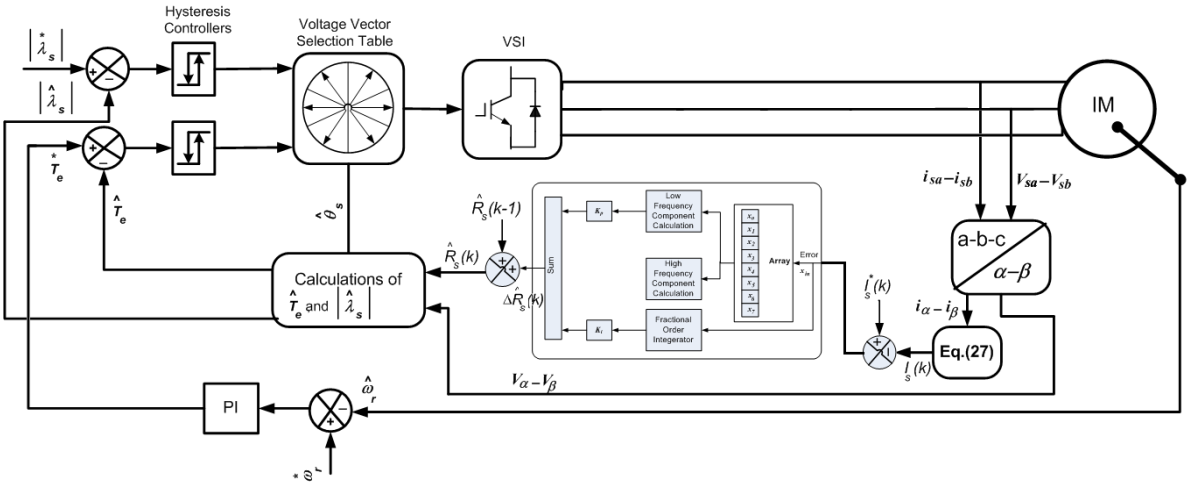

Fig. 4. Overall block diagram for DTC with the proposed stator resistance estimator.

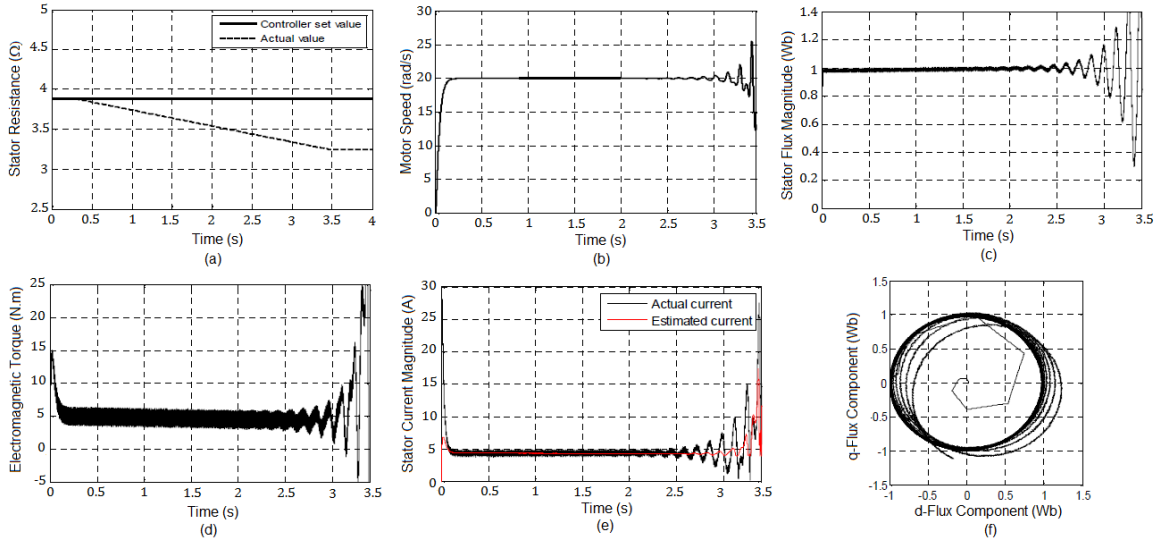

Fig. 5. Simulation results for a ramp stator resistance decrease without using resistance estimator.

5.2 DTC for IM with Multi-Resolution Wavelet PI Resistance Estimator

The proposed multi-resolution wavelet PI stator resistance estimator for the DTC IM drive has been implemented using MATLAB-SIMULINK package. Fig. 6 shows how the proposed PI estimator and its percentage of error. The estimated value of the stator resistance is precisely follows the actual value of the stator resistance. The multi-resolution wavelet PI response has the following parameters: 1- rise time is 0.21s, 2- percentage overshoot is 4.2%, and 3- steady state error is 0%.

To investigate the performance of the proposed PI stator resistance estimator, the stator resistance was changed as shown in Fig. 6(a). In this case the

actual resistance variation has a step change profile. Initially, the stator resistance is stepped up from its nominal value of 3.8 Ω to 5.7 Ω (150% of its nominal value) at t=2s. It is kept constant to 4 seconds, then it is stepped down from 5.7 Ω to 2.3Ω (60% of its nominal value) at t=6s. Fig. 6(a) shows that the estimated stator resistance has tracked its actual value in both dynamic and steady-state cases.

Moreover, the motor speed, the electromagnetic torque, the stator current, the stator flux linkages and its trajectory, shown in Fig. 6(b-f) respectively, are tracking their references very closely in the steady state. Attention to the waveforms of the flux and the torque that show that the DTC system in this case has a good performance in terms of robustness against large variations of the stator resistance. It can be seen obviously by comparing Fig. (5) by Fig. (7) that; in the steady state, the proposed method can reduce the torque ripple, current ripple, and the flux vector trajectory moves in a circle track perfectly.

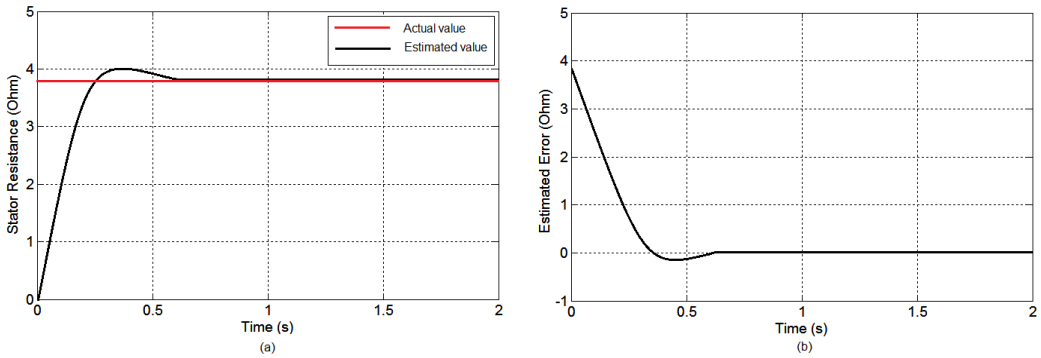

Fig. 6. Stator resistance estimation results with PI; (a) Estimated resistance, and (b) Estimation error.

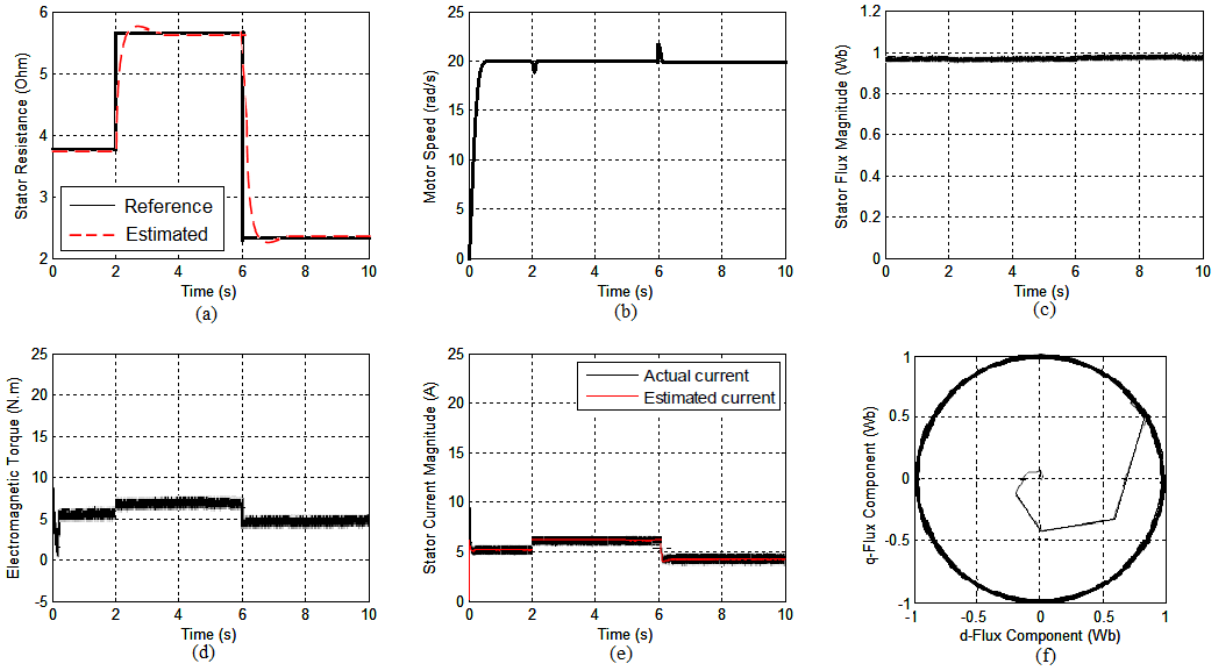

Fig. 7. Simulation results for a step change in stator resistance using multi-resolution wavelet PI resistance estimator.

6 Conclusion

The use of wavelet controller separates the high frequency components from the error input and allows the low frequency components to be processed for the determination of the proportional output. The performance of the direct torque controlled induction motor drive with wavelet stator resistance controller with the integer or fractional order integrator is introduced in this paper. The algorithm implemented for the three level wavelet decomposition is computationally far simpler as compared to the multi-resolution technique with

separate computations for high and low pass filtering at each level of decomposition. Also it is distinguished by less number of tuning constants and less tuning effort as compared to a standard multi-resolution wavelet controller. The simulation results illustrate that the proposed method can decrease the torque ripple and current ripple, superior to follow the actual value of the stator resistance for different operating conditions.

References:

[1] S. Haghhin, M.R. Zolghadri, S. Kaboli, and A. Emadi, Performance of PI Stator Resistance Compensator on DTC of Induction Motor, *IEEE Industrial Electronics Society, The 29th Annual Conference IECON '03*, 2003, pp. 425-430.

[2] F. Zidani, D. Diallo, M.E.H. Benbouzid, and R. Nait-Said, Direct Torque Control of Induction Motor With Fuzzy Stator Resistance Adaptation, *IEEE Transactions on Energy Conversion*, Vol. 21, No. 2, 2006, pp. 619-621.

[3] G. Guidi, and H. Umida, A Sensorless Induction Motor Drive For Low Speed Applications Using a Novel Stator Resistance Estimation Method, *IEEE Industry Applications Conference, The 34 IAS Annual Meeting*, 1999, pp. 180-186.

[4] E.H.E. Bayoumi, An improved approach for position and speed estimation sensorless control for permanent Magnet Synchronous motors, *Electromotion Scientific Journal*, Vol. 14, No.2, 2007, pp.81-90.

[5] E.H.E. Bayoumi, and H.M. Soliman**,** A Particle Swarm Optimization-based deadbeat on-line speed control for sensorless induction motor drives, *Electromotion Scientific Journal*, Vol. 15, No.3, 2008, pp. 141-153.

[6] B.S. Lee, and R. Krishnan, Adaptive Stator Resistance Compensator for High Performance Direct Torque Controlled Induction Motor Drives, *IEEE Industry Applications Conference, 33th IAS Annual Meeting*, 1998, pp. 423–430.

[7] E.H.E. Bayoumi, Sliding Mode Position Control of Synchronous Motor with Parameters and Load Uncertainties, *Electromotion Scientific Journal*, Vol. 17, No. 2, 2010, pp. 99-106.

[8] R.J. Kerkman, B.J. Seibel, T.M. Owan, and D.W. Schlegel, A new flux and stator resistance identifier for AC Drive systems, *IEEE Transactions on Industry Applications*, Vol. 32, No. 3, 1996, pp. 585-593.

[9] I. Ha, and S.H. Lee, An online identification method for both stator and rotor resistances of induction motors without rotational transducers, *IEEE Transactions on Industrial Electronics*, Vol.47, No. 1, 2000, pp. 842-853.

[10] L. Umanand, and S.R. Bhat, Online estimation of stator resistance of an induction motor for speed control applications, *Proc. Inst. Elect. Eng. Elect. Power Application*, Vol. 142, No. 2, 1995, pp. 97–103 .

[11] L. Liu, S. Shen, S. Liu, Q. Liu, and W. Liao, Stator Resistance Identification of Induction Motor in DTC System Based on Wavelet Network, *Proc. of IEEE the 6th World Congress on Intelligent Control and Automation*, 2006, pp. 6411- 6415.

[12] R. Marino, S. Peresada, and P. Tomei, On-line stator and rotor resistance estimation for induction motors, *IEEE Transactions on Control System Technology*, Vol. 8, No. 3, 2000, pp. 570- 579.

[13] G. Guidi, and H. Umida, A novel stator resistance estimation method for speed sensorless induction motor drives, *IEEE Transactions on Industry Applications*, Vol. 36, No. 1, 2000, pp. 1619- 1627.

[14] A. Monti, F. Pironi, F. Sartogo, and P. Vas, A new state observer for sensorless DTC control, *Proc. Inst. Elect. Eng., Power Electronics and Variable Speed Drives Conference*, 1998, pp. 311–317.

[15] B. Raison, J. Arza, G. Rostaing, and J.P. Rognon, Comparison of two extended observers for the resistance estimation of an induction machine, *Proc. IEEE Industry Applications Conference*, 2000, pp. 1330-1335.

[16] M. Tsuji, S. Chen, K. Izumi, and E. Yamada, A sensorless vector control system for induction motors using q-axis flux with stator resistance identification, *IEEE Transactions on Industrial Electronics*, Vol. 48, No. 1, 2001, pp. 185–194.

[17] K. Shinohara, T. Nagano, and W.Z.W. Mustafa, Online tuning method of stator and rotor resistances in both motoring and regenerating operations for vector controlled induction machines, *Electrical Engineering in Japan Journal*, Vol. 135, No. 1, 2001, pp. 56-64.

[18] KARANAYIL, B. "Parameter identification for vector controlled induction motor drives using artificial neural networks and fuzzy principles", A PhD thesis, School of Electrical Engineering and Telecommunications, University of New South Wales, 2005.

[19] E.H.E. Bayoumi, Parameter Estimation of Cage Induction Motors Using Cooperative Bacteria Foraging Optimization, *Electromotion Scientific Journal*,Vol.17, No.4, 2010, pp.247-260.

[20] E.H.E. Bayoumi, M. Awadallah, and H.M. Soliman, Deadbeat performance of vector-controlled induction motor drives using particle swarm optimization and adaptive neuro-fuzzy inference systems, *Electromotion Scientific Journal*, Vol.18, no. 4, 2011, pp. 231-242.

[21] L.A. Cabrera, E. Elbuluk, and I. Husain, Tuning the stator resistance of induction motors using artificial neural network, *IEEE Transactions on Power Electronics*, Vol.12, No. 5, 1997, pp. 779–787.

[22] M. Awadallah, E.H.E. Bayoumi, and H.M. Soliman, Adaptive deadbeat controllers for BLDC drives using PSO and ANFIS techniques, *Journal of Electrical Engineering*, Vol 60, No. 1, 2009, pp. 3-11.

[23] J. Campbell, and M. Sumner, Practical sensorless induction motor drive employing an artificial neural network for online parameter adaptation, *Proc. Inst. Elect. Eng., Elect. Power Applications*, Vol. 149, No. 4, 2002, pp. 255–260.

[24] B.K. BOSE, and N.R. PATEL, Quazi-fuzzy estimation of stator resistance of induction motor, *IEEE Transactions on Power Electronics*, Vol. 13, No. 3, 1998, pp. 401–409.

[25] S.-J. Steven Tsai, *Power transformer partial discharge (PD) acoustic signal detection using fiber sensors and wavelet analysis, modeling, and simulation*, Master's Thesis, Electrical and Computer Engineering, Virginia Polytechnic Institute and State University, Chapter 4, 2002.

[26] A.S Sant, and K. R.Rajagopal, PM Synchronous Motor Drive with Wavelet Controller and Fractional Order Integrator, *Power Electronics,and Energy Systems (PEDES 2010), New Delhi*, 2010, pp.1-8.

[27] L. Liu, S. Shen, S.Liu, Q. Liu, , and W. Liao, Stator resistance identification of induction motor in DTC system based on wavelet network, *Proc. Intelligent Control and Automation*, Dailian, China, 2006, pp.6411-6415.

[28] S. Parvez and Z. Gao, A wavelet-based multiresolution PID controller, *IEEE Transaction on Industrial Applications.*, Vol. 41, No.2, 2005, pp. 537-543.

[29] E. Mitronikas and E. Tatakis, Design of a wavelet multiresolution controller for speed control of travelling wave ultrasonic motors, *Proc. 2008 IEEE Power Electronics Specialists Conference*, pp.3937-3942, 2008 .

[30] M. A. S. K. Khan, and M. A. Rahman, Implementation of a New Wavelet Controller for Interior Permanent Magnet Motor Drives, *Record of the 2007 IEEE Industry Applications Conference, 42nd IAS Annual Meeting*, pp.1280 – 1287, 2007.

[31] Bayoumi, E.H.E. "A novel approach to control an unbalanced three phase induction motor", *Electromotion Scientific Journal* , Vol 12, No.4, pp.213-222, 2005.